INTERNATIONAL JOURNAL OF ENERGY RESEARCH
Int. J. Energy Res. 2009; **33**:696–708
Published online 30 December 2008 in Wiley InterScience
(www.interscience.wiley.com). DOI: 10.1002/er.1505

A numerical analysis of energetic performances of active and passive aftertreatment systems

Angelo Algieri, Mario Amelio and Pietropaolo Morrone*,†

Mechanics Department, University of Calabria-87030, Arcavacata di Rende (CS), Italy

SUMMARY

The present work aims to analyze the thermal and the energetic performances of an aftertreatment system with unidirectional and periodic reversal flow within the device. To this purpose a single-channel one-dimensional model was developed in order to assess the heat exchange between the aftertreatment system and the exhaust gas. Furthermore, the temperature profiles of the gas and solid phase were computed and the calculated temperatures were adopted to characterize the energy effectiveness of the aftertreatment system. The comparison between different control modes showed an increase in the heat retention efficiency of the system with reverse flow at low engine load conditions. Conversely, the system with passive thermal management presented higher temperatures of the monolith during the warm-up operations. Furthermore, the influence of unburned hydrocarbons oxidation on the effectiveness of the aftertreatment system was evaluated and the significant influence of the cycle time and the monolith length on the system performance was shown. Finally, the gas residence time was evaluated for different operating conditions.

KEY WORDS: aftertreatment systems; active and passive flow control; numerical analysis

1. INTRODUCTION

Nowadays the development and the optimization of aftertreatment systems are fundamental keys to meet the ever more severe regulations concerning automotive exhaust emissions [1–6]. In the last few decades a host of experimental and numerical investigations have been carried out to increase the efficiency of aftertreatment systems and reduce engine tail pipe emissions [7–12]. Attention has been mainly focused on three-way catalysts (TWCs), oxidation catalysts (OCs), diesel particulate filters (DPFs), lean NO_x traps (LNTs), lean NO_x catalysts (LNCs) and selective catalytic reductions (SCRs) [13–17]. Specifically, a host of investigations demonstrated that, for stoichiometric spark ignition engines, three-way catalytic converters represent a proper and efficient method to control the pollutant emissions, as can be found in literature [7,18–20].

Conversely, for the lean burn engine, energy-efficient technologies to treat simultaneously nitrogen oxides (NO_x), particulate matters (PM), carbon monoxide (CO) and hydrocarbons (HC)

*Correspondence to: Pietropaolo Morrone, Mechanics Department, University of Calabria-87030, Arcavacata di Rende (CS), Italy.
†E-mail: pp.morrone@unical.it

Received 22 July 2008
Revised 12 November 2008
Accepted 18 November 2008

are not available, and an integration of different aftertreatment systems is often necessary [6,21,22]. In fact, the large amount of oxygen in exhaust gas negates the use of TWCs. Furthermore, the low temperatures of the exhaust gas in the lean burn engine, usually, impose the addition of supplemental fuel in order to guarantee the proper thermal level for standard aftertreatment systems. As a consequence, a not negligible fuel penalty and a deleterious impact on engine energy efficiency are produced. In particular, high temperatures are required to regenerate diesel particulate filters to initiate and to sustain light-off condition for OCs and to permit the desulfurization process for LNTs [21,23]. Following Johnson [6], about 50–70% NO_x treatment on heavy-duty (HD) diesel engines will be needed at 500–520°C to meet US NTE (not-to-exceed) regulations, introduced by the United States Environmental Protection Agency (US EPA).

Also SCRs can demand high operating temperatures, depending both on the base oxides/metals used as active catalysts and on the reducing agents. As an example, Burch *et al.* showed that alumina is very active for C_3H_6-*SCR* and selective to NO_x but only at high temperatures (i.e. above 400°C), while the adoption of silver promoted alumina catalyst significantly reduces the requested thermal level [19].

On the other hand, SCR with urea offers attractive solutions at low temperature and, often, serious aging and durability problems appear when high temperature conditions are imposed [24]. Similar results were found when LNTs are used for light-duty (LD) applications with traditional diesel combustion [6].

Furthermore, a review of the literature reveals that all the aftertreatment systems require proper operating temperatures and an accurate flow control to guarantee reliable and efficient processes.

To this purpose, in the last few years, an innovative active flow control has been proposed to assure the correct thermal window for energy-efficient aftertreatment operations and to reduce the addition of supplemental fuel [21,25].

The new strategy is based on reversed flow systems and, additionally, on the control of the exhaust gas flow path through the aftertreatment apparatus (Figure 1). Specifically, the exhaust gases are periodically switched between the two system ends by means of valves [26]. A cycle consists of forward and backward operations. The cycle is defined as symmetric reverse flow if the two consecutive processes last the same time, otherwise the cycle is termed as asymmetric reverse flow.

The present work aims to compare the thermal and, as a consequence, the energetic performances of a generic aftertreatment system with and without flow inversion (passive and active flow control, respectively). In fact, several studies on aftertreatment systems exist in the literature, while few studies refer to active flow control. The analysis is focused on the thermal behavior of the system to compare different flow control modes and to quantify the response of the aftertreatment system after sudden variations in engine load. As a consequence, the catalytic reactions are not taken into account and the

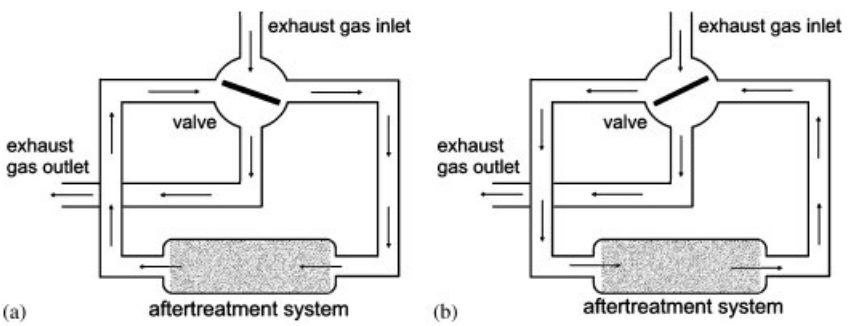

Figure 1. Active aftertreatment system: forward (a) and backward (b) operations.

DOI: 10.1002/er

results can be extended to a generic aftertreatment system with structured packed bed.

As an original contribution to the thermal analysis, two indices (the *Stored Energy Fraction—SEF* and the *Percentage Residence Time—PRT*) were introduced. Specifically, the dimensionless SEF was defined to compare different flow control modes, independently of the operating conditions, while the residence time was introduced to evaluate the length of time that the gas temperature is in a fixed thermal window. Particularly, the residence time takes into account the actual temperature profiles within the aftertreatment system and it was calculated referring to different thermal windows.

Finally, the effect of the cycle time, the monolith length and the exothermic reactions of the unburned HC in the exhaust gas were analyzed.

2. NUMERICAL MODEL

A one-dimensional single-channel transient model was used to simulate the thermal exchange between the exhaust gas and the aftertreatment system, in this case a structured monolith, which usually consists of bricks having longitudinal square holes with about 1 mm × 1 mm cross flow area. A typical cross section of the monolith bed is shown in Figure 2, while the dotted square represents the control volume adopted in the model.

The proposed numerical code simulates the thermal exchanges inside a single channel of the aftertreatment system. The basic model assumptions are the following:

- working fluid as ideal mixture;
- one-dimensional unsteady flow;
- constant mass flow rate;
- negligible thermal accumulation of the gas in the monolith;
- negligible conductive and radiative energy exchange mechanisms;
- adiabatic systems towards the surroundings.

In accordance with the literature [27], the composition of the exhaust gas was calculated from the combustion of $C_{12}H_{24}$ with excess air. The oxidation of the unburned HC present in the working gas was treated by assuming an equivalent mass flow rate of methane, that is, representative of the combined exhaust HC and CO in average diesel and lean burn gaseous fuel engines, in accordance to literature [21].

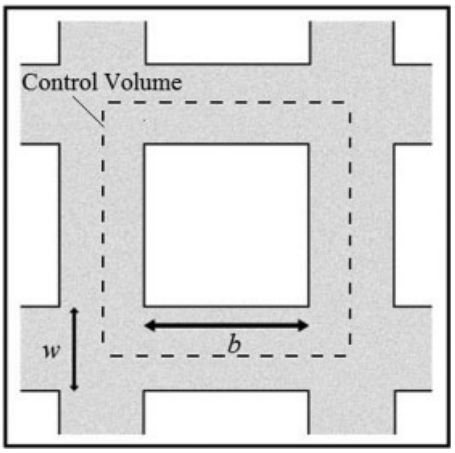

Figure 2. Typical cross section of a structured converter.

Referring to the control volume, the thermal exchange can be described as follows:

$$\frac{\partial T}{\partial x} = \frac{h \cdot (P/A_c) \cdot (T_s - T)}{G \cdot c_p} \tag{1}$$

where h is the heat transfer coefficient, x is the longitudinal coordinate, P is the channel perimeter, A_c is the cross area of a single channel, T is the gas temperature, T_s is the solid temperature, G is the mass flow rate per unit area A_c, c_p is the specific heat of the working fluid.

The ratio (P/A_c) is the exchange surface per unit volume of the bed and $S\,dx$ is the volume of solid that exchanges thermal energy with the gas:

$$S = w \cdot (2b + w) \tag{2}$$

where b and w are visible in Figure 2.

The monolith temperature was calculated according to the following energy balance for the solid phase:

$$\rho_s \cdot c \cdot S \cdot dx \cdot \frac{\partial T_s}{\partial t} = \dot{q}_{exoth} \cdot P \cdot dx - G \cdot A_c \cdot c_p \cdot dT \tag{3}$$

DOI: 10.1002/er

where c is the specific heat of the solid phase, ρ_s is the solid density, t is the generic time, $\dot{q}_{exoth}$ is the exothermic energy generation rate per unit area, related to the oxidation of the equivalent methane.

The exothermic reaction of the working fluid was treated as surface heat generation. Conversely, the effect of reactions in the gas phase was ignored. The energetic contribution of oxidation was equally distributed over the whole channel:

$$\dot{q}_{exoth} = \frac{\dot{m}_{CH_{4Eq}} \cdot LHV}{P \cdot L} \tag{4}$$

where LHV is the lower heating value, L is the monolith length, $\dot{m}_{CH_{4Eq}}$ is the equivalent methane mass flow rate.

For the complete resolution of the problem, the following equations were considered:

$$\frac{\partial(\rho v)}{\partial x} = 0 \tag{5}$$

$$\frac{\partial p}{\partial x} = -\frac{1}{2 \cdot D_{eq}} \cdot f \cdot \rho \cdot u^2 \tag{6}$$

$$p = \rho \cdot R^* \cdot T \tag{7}$$

where v is the gas velocity, ρ is the gas density, p is the gas pressure, D_{eq} is the channel hydraulic diameter.

The momentum balance equation for a fixed bed is taken into account through Equation (6). It depends on the Fanning coefficient f, equal to 64/Re for laminar flow (Re < 2000), as that occurs in the operative conditions of this paper.

The equations were solved with a finite difference scheme. More detail on the model and on the relative validation are reported in the literature [28–30]. As far as the heat transfer coefficient is concerned, various correlations are present in the literature. Specifically, there are correlations for laminar or turbulent flow, for constant heat flux or constant solid temperature [31,32]. The heat transfer coefficient h was obtained as a function of Reynolds (Re) and Prandtl (Pr) numbers, using the correlation attributed to Hausen [33] and adopted by Rafidi and Blasiak [34] to study the thermal exchange within a structured monolith:

$$\begin{aligned} Nu &= h \cdot D_{eq}/k \\ &= 3.61 + \frac{0.0668 \cdot (D_{eq}/L) Re\ Pr}{1 + 0.04 \cdot [(D_{eq}/L) Re\ Pr]^{2/3}} \end{aligned} \tag{8}$$

The value of the Nusselt number for the operating condition used in the present work is near to 3.65, while 3.66 is the Nu constant value largely adopted in the literature for square cross section and constant heat flux with a fully developed laminar flow [31,32].

3. OPERATIVE CONDITIONS AND PERFORMANCE PARAMETERS

The model was applied to an aftertreatment system, whose operating conditions (typical of a HD diesel) are shown in Table I [21].

To analyze the energy performance of the aftertreatment system, a '*cooling*' and a '*heating*' process were analyzed. In particular, during the '*cooling*' phase, gas enters into the system at 200°C, while the initial solid temperature is 700°C. This corresponds to a sudden decrease in the engine load after prolonged full load operation.

Therefore, at the beginning of the process, the aftertreatment system presents a maximum internal energy value:

$$E_{max} = m \cdot c \cdot T_{s,0} \tag{9}$$

Table I. Operative conditions for the aftertreatment system and the working fluid.

Reference converter size (mm) (*height* × *width* × *length*)	141 × 141 × 300	
Further converter lengths (mm)	200, 400, 500, 600	
Cell density (cell cm^{-2})	62	
Solid phase density (kg m^{-3})	2807	
Channel size (mm)	$b = 0.90$	
	$w = 0.35$	
Solid specific heat (J kg^{-1} K^{-1})	800	
Exhaust flow rate (g s^{-1})	100	
Methane mass flow rate (g s^{-1})	0.15	
Inlet gas temperature (°C)	200	(700)
Initial solid temperature (°C)	700	(200)
Cycle time (s)	10–100	

DOI: 10.1002/er

where m is the monolith mass and $T_{s,0}$ is the initial temperature of the solid.

For simplicity, the internal energy is assumed zero when the temperature is equal to 0 K. The low temperature gas flow determines the progressive cooling of the solid. Specifically, the minimum energy state corresponds to the complete cooling of the aftertreatment system:

$$E_{\min} = m \cdot c \cdot T_{\text{gas inlet}} \tag{10}$$

where $T_{\text{gas inlet}}$ is the inlet gas temperature.

During the 'heating' process, the inlet gas temperature is equal to 700°C, while the solid is at 200°C. At the beginning of the process, the aftertreatment apparatus presents a minimum internal energy value:

$$E_{\min} = m \cdot c \cdot T_{s,0} \tag{11}$$

The high temperature gas flow determines the gradual heating of the solid. The corresponding maximum energy is:

$$E_{\max} = m \cdot c \cdot T_{\text{gas inlet}} \tag{12}$$

3.1. Stored energy fraction (SEF)

The evaluation of the aftertreatment system thermal performance was achieved through a new parameter, the SEF:

$$\text{SEF} = \frac{E(t) - E_{\min}}{E_{\max} - E_{\min}} \tag{13}$$

where $E(t)$ is the thermal energy stored in the solid at time t:

$$E(t) = \frac{m \cdot c \cdot \int_0^L T_s(x,t) \cdot \mathrm{d}x}{L} \tag{14}$$

The fraction of the stored thermal energy is a function of time, and it assumes values between 0 and 1 for both operating conditions (cooling and heating process). The parameter decreases from one to zero during the cooling process, and thus represents a heat retention efficiency.

Conversely, during the heating phase, the SEF raises from zero to unity. In this case the dimensionless parameter represents an efficiency index of the heating process.

The SEF parameter permits to compare the thermal characteristics of different aftertreatment systems (active and passive flow control), independently of the operating conditions (i.e. inlet gas temperature, initial solid temperature) and to evaluate the system response to fast variations in the engine load.

3.2. Percentage residence time

The *SEF* parameter is related to the thermal performance of the solid material, but it does not provide any information on the gas temperature and the proper thermal window that are requested to guarantee reliable and efficient aftertreatment processes. As a consequence, a new parameter that characterizes the gas phase is also useful. To this purpose, the PRT was defined as follows:

$$\text{PRT} = \frac{\bar{t}}{\text{MRT}} \cdot 100 \tag{15}$$

where $\bar{t}$ represents the length of time that the gas stays in the monolith within a fixed thermal window ($T_1 \leqslant T \leqslant T_2$) for each semi-cycle:

$$\bar{t} = \frac{\int_0^{t_{\text{cycle}}/2} \int_0^L \dfrac{a(T)}{v(x,t)} \,\mathrm{d}x \,\mathrm{d}t}{(t_{\text{cycle}}/2)} \tag{16}$$

where $a(T) = 1$ if $T_1 \leqslant T \leqslant T_2$, while $a(T) = 0$ elsewhere.

The mean residence time (MRT) can be calculated from Equation (16), considering always $a(T) = 1$.

The proper temperature range is crucial to assure a reliable and efficient aftertreatment process. Specifically, the requested temperature strongly depends on the characteristics of the particular aftertreatment system and on the relative chemical reactions that are beyond the purposes of the present work.

4. RESULTS

The one-dimensional single-channel model was used to predict the SEF of an aftertreatment system with and without reverse flow (active and passive flow control respectively). Furthermore, the effects of the cycle time and the HC oxidation were also analyzed. Specifically, for the active flow control mode, a symmetrical thermal cycle was

DOI: 10.1002/er

studied (the forward and reverse flow time are the same).

Figure 3 shows the evolution of temperature profiles of gas and solid phase along the monolith as a function of time. The figure refers to the passive flow control mode, neglecting the oxidation contribution. The initial temperature of the solid is set equal to 700°C while the inflow gas temperature is 200°C. This operating condition simulates the exhaust gas at low load conditions [21].

The analysis reveals the great influence of time on the temperature distribution within the monolith. The leading part of the aftertreatment system is almost completely cooled after 25 s, while at the outlet, the temperature values are close to 700°C. Furthermore, the solid appears thoroughly cooled after 100 s. A similar behavior is observed for the gas phase. Specifically, the temperature differences between the gas and solid phase tend to reduce with the operating time and the maximum percentage differences move from about 10% at 25 s to about 1% at 100 s.

The evolution of solid temperature profiles with the active control system in a range of 100 s is illustrated in Figure 4. The cycle time is 20 s, and the energy contribution of oxidation is also neglected. Specifically, the bold lines correspond to the time values reported in Figure 3 for an operating time greater than 20 s. Furthermore, in order to show the progress of the thermal wave inside the solid phase, the temperature profiles at the beginning and at the end of each inversion are represented (four cycles were reported). The analysis evidenced that the reverse flow operation determines a different temperature distribution within the aftertreatment system. A maximum temperature value is located at the central region of the system, with a progressive decrease from about 663°C at 25 s to 460°C at 100 s. The temperature of the two boundary regions of the monolith is always near to the inflow gas one (200°C).

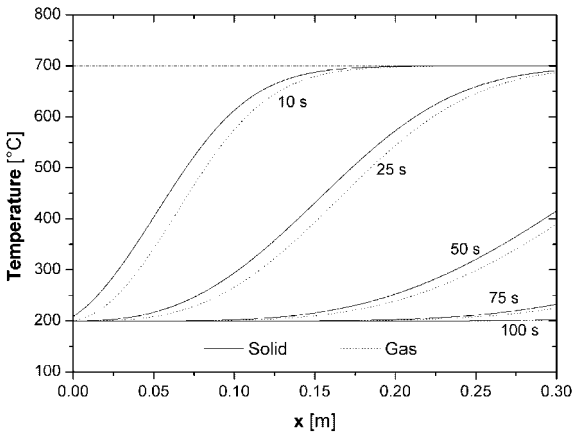

Figure 3. Temperature profiles of the gas and solid phase along the aftertreatment system as a function of time. Passive control and cooling phase.

The comparison with the results obtained with conventional unidirectional flow shows, therefore, the greater thermal retention capacity of the active aftertreatment system. In particular, for the passive control system, the solid phase is almost completely cooled after 100 s. Conversely, the active control allows one to maintain significantly higher temperature values in the monolith central area, with an increase of about 260°C. When high temperatures are required, the reverse flow control determines the maintenance of suitable temperatures for the proper operation of the aftertreatment system, even under lean mixture conditions and low load operation, without additional fuel. Therefore, the active technique permits a significant energy savings with respect to the passive control strategy [21].

Figure 5 depicts the comparison between the SEF for both the control modes, neglecting the oxidation effect. The analysis confirms that, after 100 seconds, the thermal retention effectiveness of the system without reversing flow falls to zero, while a value of nearly 37% is found when the active control is used. In this case, the SEF of the system becomes 3% after about 400 seconds (20 cycles).

The effect of the inlet gas temperature on the stored thermal energy fraction, for the cooling phase is shown in Figure 6. Specifically, the plot refers to 3 different gas temperature values: 200, 400 and 600°C. For the first 40 s (2 cycles) the difference in the thermal behavior is negligible, while some variation was found in the range 40–500 s. Nevertheless, the differences affecting the SEF parameter between 200 and 600°C are always

DOI: 10.1002/er

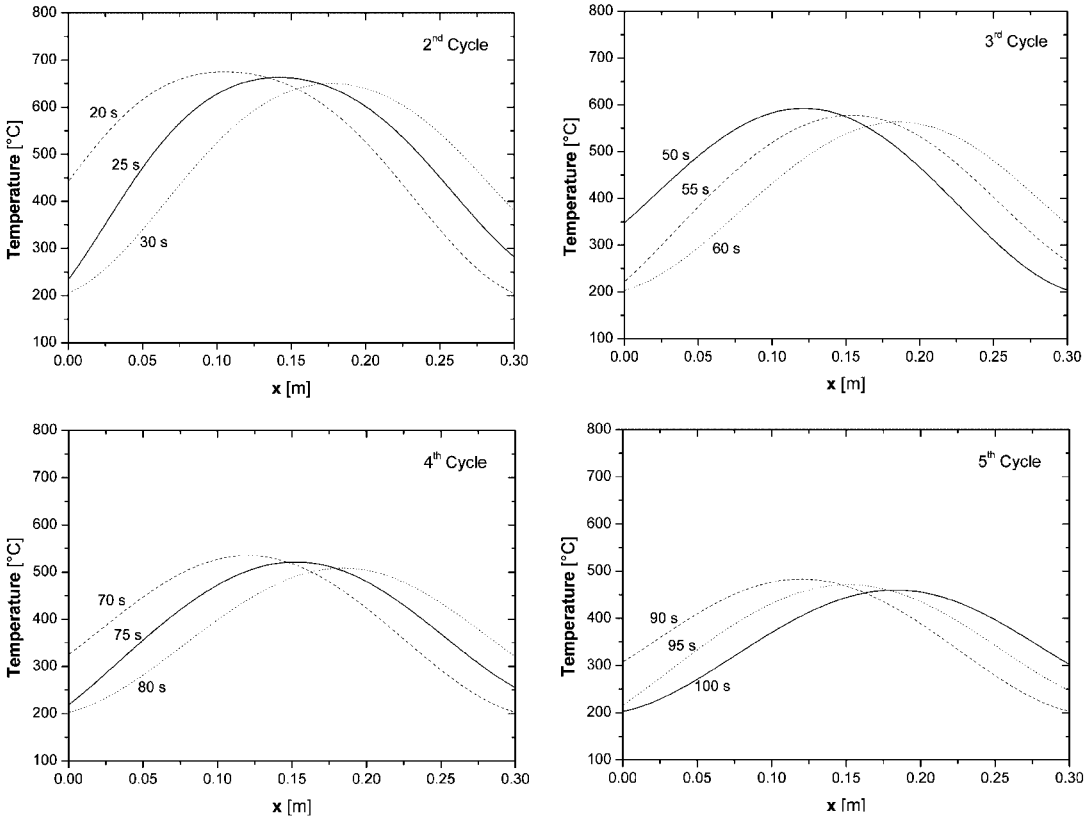

Figure 4. Solid temperature profiles along the aftertreatment system as a function of time. Total time: 100 s, time cycle: 20 s. Active control and cooling phase.

lower than 0.03. The inlet gas temperature is fundamental to assure the proper thermal window and a reliable and efficient aftertreatment process. However, the analysis revealed that the dimensionless SEF parameter is roughly independent of the temperature of the inlet gas. As a consequence, to design and optimize an efficient aftertreatment system, attention should be focused on other parameters, such as the geometry or the thermo-physic properties of the material.

For the reversed flow control, the gas residence time in specific temperature windows was evaluated. The accurate knowledge of the residence time is, in fact, a fundamental key to control the aftertreatment processes. Figure 7 depicts the MRT as a function of the cycle number (continuous line) and the residence time of the gas above 300, 400 and 500°C (scattered data). The cycle time is 20 s. As expected, MRT

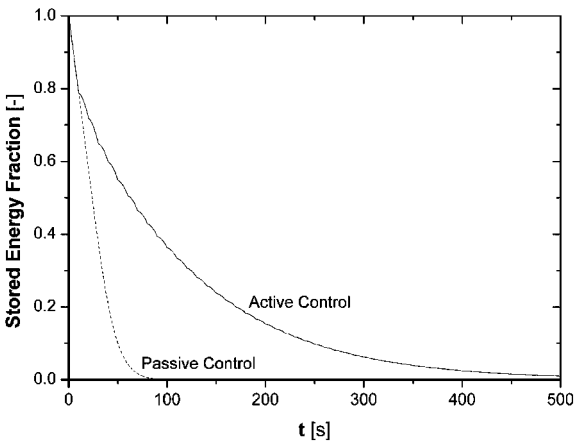

Figure 5. Stored thermal energy fraction with active and passive flow control.

increases and residence times reduce with the cycle number due to the gas temperature decrease.

DOI: 10.1002/er

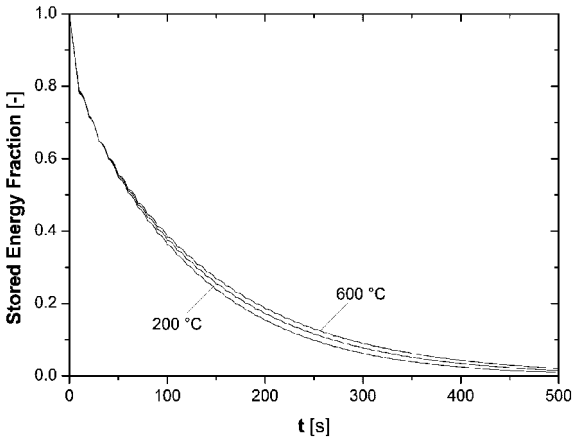

Figure 6. Inlet gas temperature effect on the stored thermal energy fraction. Active control. Cycle time 20 s. Cooling phase.

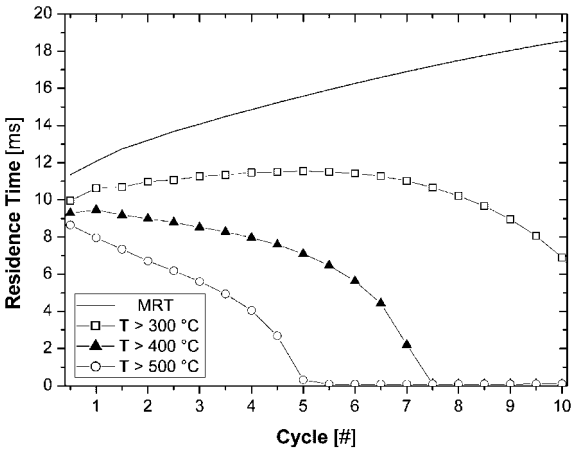

Figure 7. Residence time as a function of the number of cycles.

Moreover, the higher the threshold temperature, the lower the residence time. As an example, at the 6th cycle the residence times are 11.43, 5.63 and 0.09 ms for the gas temperature above 300, 400 and 500°C, respectively.

The PRTs for three thermal levels ($T>300$°C, $T>400$°C, $T>500$°C) are plotted in Figure 8. For the sixth cycle the PRT approaches zero for $T>500$°C, whereas it is 35% for $T>400$°C and 70% for $T>300$°C.

In order to analyze the effect of the reversal flow control in more detail, the comparison between active and passive mode was repeated considering the solid heating process (Figure 9). Specifically, the solid initial temperature is set equal to 200°C and the temperature of exhaust gases to 700°C. This condition corresponds to high load engine operation after a long period of low load operation. As already observed, when passive control is adopted (Figure 9(a)), the monolith leading region is almost completely heated after 30 seconds, while the opposite end retains temperature values close to 200°C. However, after 100 seconds, the aftertreatment system appears totally heated, at temperatures close to 700°C.

Figure 9(b) shows the temperature profiles with the reverse flow during the heating process. The comparison with the previous results highlights a greater thermal inertia of the active control system

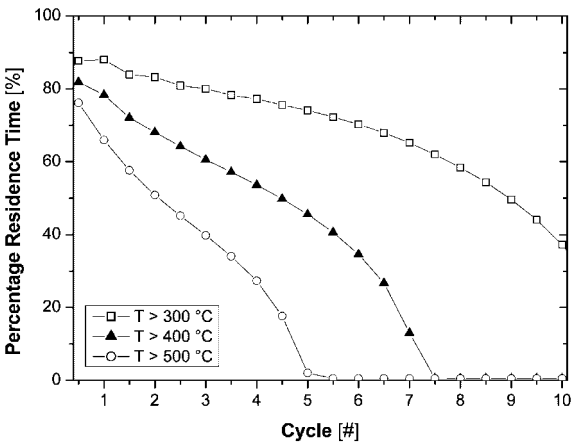

Figure 8. Percentage residence time (PRT) as a function of the number of cycles.

and therefore a greater delay in reaching a high heat level. Specifically, after 100 s the temperature in the central part of the aftertreatment system is lower than 440°C.

The stored thermal energy fraction confirms the results already discussed. In particular, the system with passive control allows the achievement of SEF = 1 after about 70 seconds, while the reversed flow control presents SEF $\approx$ 0.54.

The analysis demonstrates that, if high temperatures are required for the proper functioning of the aftertreatment system, the active control is useful at low load operating

DOI: 10.1002/er

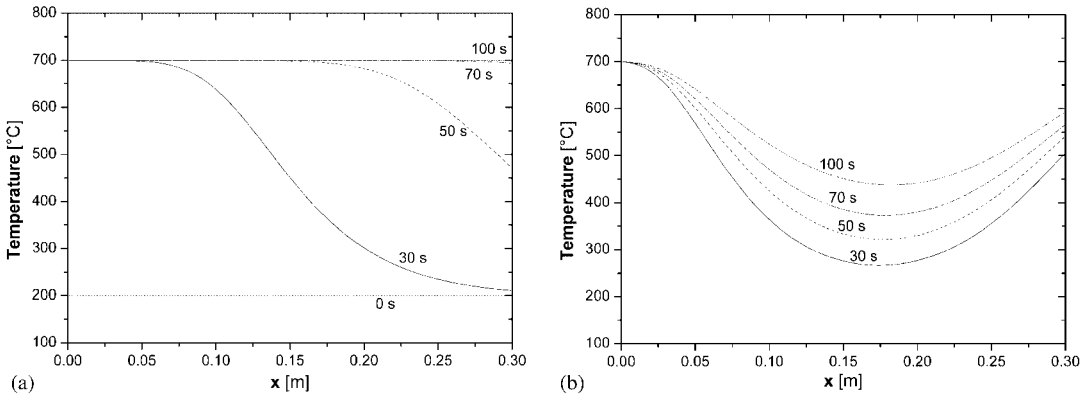

Figure 9. Temperature profiles of the solid phase along the aftertreatment system as a function of time with (a) passive and (b) active control. Heating phase.

condition with the monolith at high temperature. The reversal mode allows to reduce or avoid the supplemental fuel which has a negative impact on the engine energy efficiency. Active control could be an attractive solution also if low temperature operations are requested. The higher thermal inertia of the reversal mode permits, in fact, the maintenance for a longer time of the initial temperature level in the aftertreatment system after sudden variations in engine load. Conversely, the passive control system is recommended during the warm-up phase and/or to accelerate the cooling or the heating process.

4.1. Effect of oxidation

The following analysis is restricted to the cooling phase (inlet gas temperature: 200°C, initial solid temperature: 700°C).

Figure 10 shows the evolution of the solid temperature profiles with active control, with a semi-cycle period of 10 s. The energy contribution of the unburned HC oxidation is taken into account. The oxidation effect on temperature profiles is not negligible, and a growing influence over time operating is observed. In fact, it should be noted that the weight of the energy exothermic reaction increases with the number of reversals as a result of the exchange convective heat decrease. As an example, the differences between the maximum temperature values with and without the effect of the oxidation are about 37, 72, 92 and 153°C for the second, third, fourth and fifth cycle respectively.

The effect of the retention effectiveness for active and passive control is visible in Figure 11. For a long time of operation, when the convective thermal exchange becomes negligible, SEF does not tend to zero due to the energy oxidation effect. Specifically, the active control system presents a 18% higher SEF value with respect the passive flow control due to the better thermal retention characteristic of the reverse operation. Conversely, as already observed, the effectiveness for active and passive control tends to the same value (zero) without the oxidation.

4.2. Effect of cycle time

In order to explore in more detail the influence of the control mode on the aftertreatment system heat retention, a parametric study of the effect of the cycle time was carried out (Figure 12). Specifically, the cooling phase is considered. The SEF curves, related to the active control aftertreatment systems, are catenary. Moreover, the figure shows the presence of peaks associated with the switching time.

Furthermore, Figure 12 illustrates that the performance of the aftertreatment system with active flow control approaches the curve corresponding to the passive control as the cycle time increases. Specifically, before the first reversal (during the first semi-cycle) the system with active flow control behaves as a passive aftertreatment

DOI: 10.1002/er

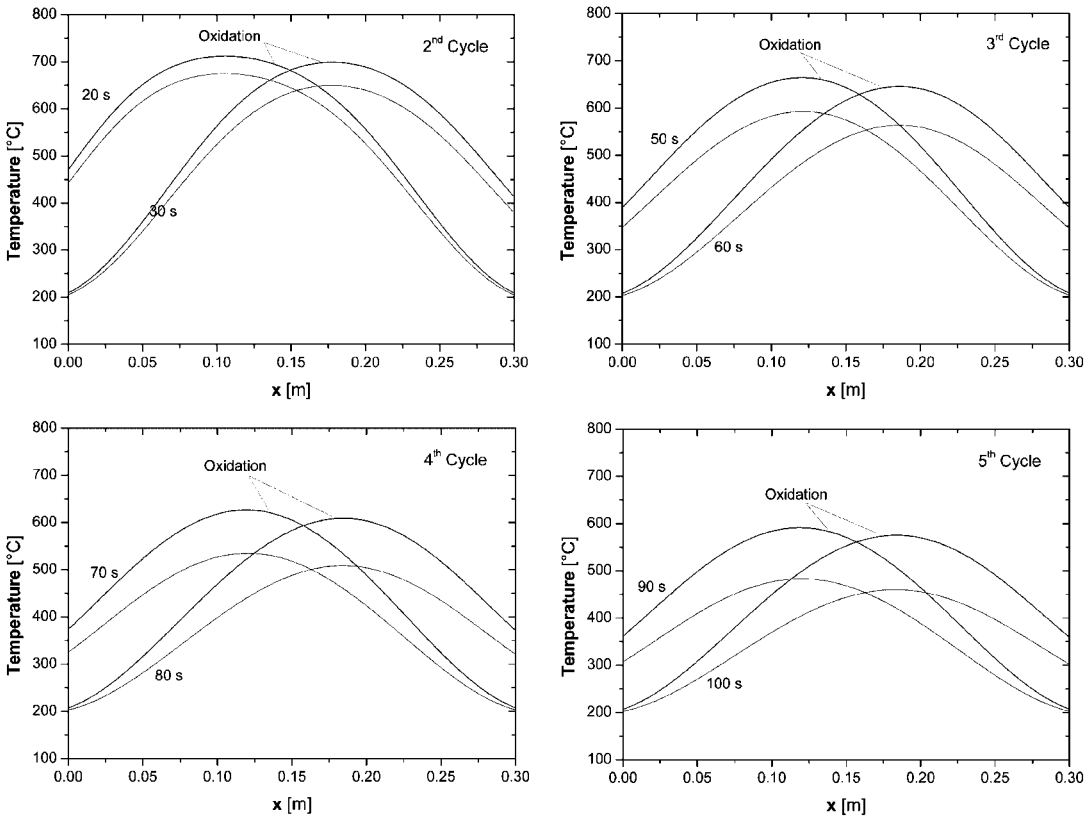

Figure 10. Temperature profiles of the solid phase along the aftertreatment system as a function of time, with oxidation. Active control and cooling phase.

apparatus and the two relative curves coincide. As a consequence, higher the cycle time value, higher the curve drop.

4.3. *Effect of monolith length*

The great influence of the aftertreatment system length on the SEF, for the cooling phase is shown in Figure 13. The plot refers to five monolith lengths (from 0.2 to 0.6 m—Table I) for the cooling process. For a fixed operating time, the higher the monolith length, the higher the retention efficacy. As an example, after 300 s, the shortest monolith ($L = 0.2$ m) retention efficacy falls to zero, while the 0.6 m aftertreatment system preserves a great thermal retention capacity, with a SEF value higher than 0.40.

Finally, the effect of the monolith length on the MRT is reported in Figure 14. The residence time

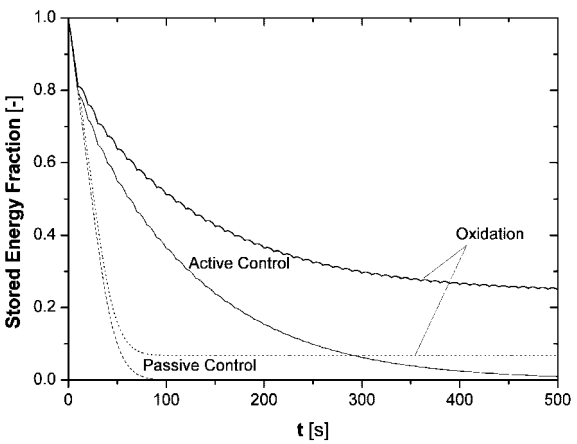

Figure 11. Influence of the oxidation on the stored thermal energy fraction with active and passive flow control. Heating phase.

DOI: 10.1002/er

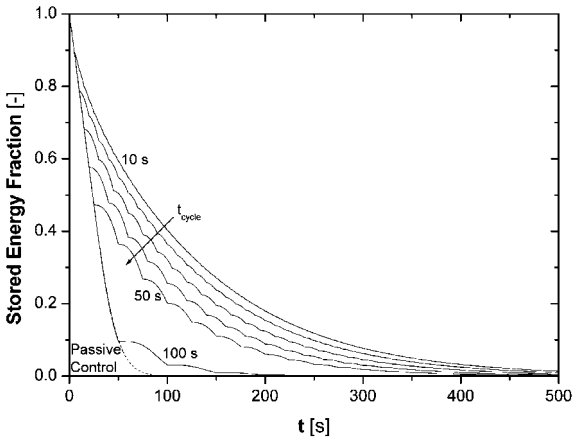

Figure 12. Stored thermal energy fraction with active and passive flow control.

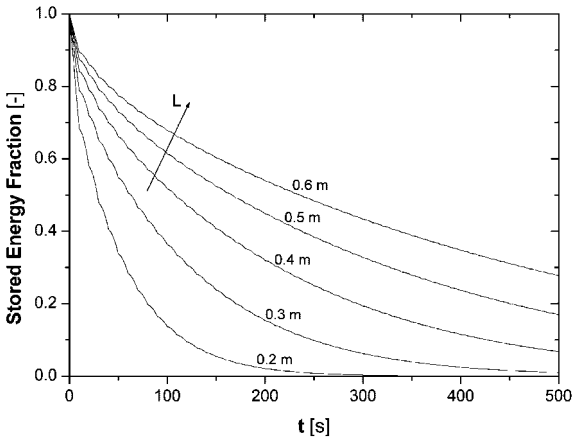

Figure 13. Converter length effect on the stored thermal energy fraction. Cycle time: 20 s. Active control and cooling phase.

is proportional to the length of the aftertreatment system for the first cycles. As the number of inversions increases, the proportionality is lost and a sudden drop is observed for all the curves. Specifically, the decreasing rate is lower as the aftertreatment size increases.

5. CONCLUSIONS

A single-channel one-dimensional model is proposed in order to analyze the thermal performance

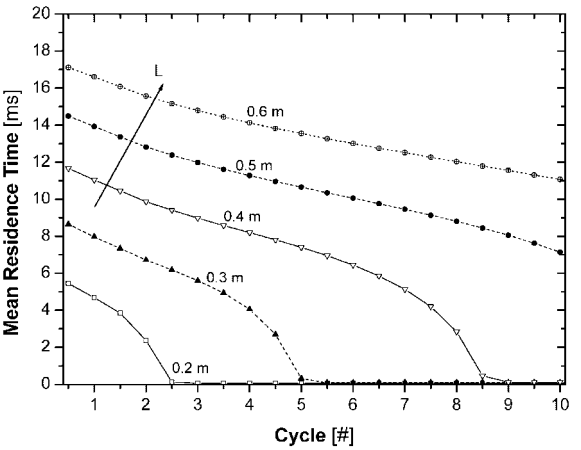

Figure 14. Converter length effect on the mean residence time (MRT). Cycle time: 20 s. Active control and cooling phase.

of an aftertreatment system, and to evaluate the influence of the key operating parameters on the process characteristics. Specifically, the code enables the calculation of the heat exchange between the solid and the gas, and the determination of the gas and solid phase temperature profiles. The analysis was carried out considering both passive and active flow control. The latter is based on periodic reversal of flow through the aftertreatment system. The temperature profiles of solid phase were used for the characterization of the SEF, while the gas temperature profiles were adopted for the evaluation of the mean and PRT.

The comparison between active and passive flow control showed the greatest thermal inertia of reversal operation. As a consequence, the reversed flow controls appear more suitable to maintain the monolith initial temperature level for a longer time after sudden variations in engine load. Conversely, if rapid 'cooling' or 'heating' of the solid phase are requested, the unidirectional flow is preferable.

Furthermore, the analysis showed that the effect of the HC oxidation on the temperature profiles is not negligible. Specifically, its influence increases with the cycle number.

The study demonstrated the significant influence of the cycle time on the system during the 'cooling' phase. In particular, the energy

DOI: 10.1002/er

performances of the active control system asymptotically approaches those of the passive control system as the cycle time increases.

Finally, the numerical analysis evidenced the great influence of the aftertreatment system length on the stored thermal energy fraction and on the MRT. Specifically, the retention efficacy and the residence time increase as the monolith length rises.

NOMENCLATURE

A_c	= channel cross area
c_p	= specific heat of the gas
C	= specific heat of the solid phase
CO	= carbon monoxide
D_{eq}	= channel hydraulic diameter
DPF	= diesel particulate filter
$E(t)$	= thermal energy at time t
ε	= stored energy fraction
F	= fanning friction coefficient
G	= mass flow rate per unit area A_c
H	= heat transfer coefficient
HC	= hydrocarbons
L	= converter length
LHV	= lower heating value
LNC	= lean NO_x catalyst
LNT	= lean NO_x trap
m	= monolith mass
$\dot{m}_{CH_{4Eq}}$	= methane equivalent mass flow rate
MRT	= mean residence time
NO_x	= nitrogen oxides
NTE	= not to exceed
OC	= oxidation catalyst
P	= channel perimeter
PM	= particulate matter
PRT	= percentage residence time
$\dot{q}_{exot}$	= exothermic energy generation rate
SCR	= selective catalytic reduction
SEF	= stored energy fraction
t	= time
T	= gas temperature
T_s	= solid temperature
$T_{gas\ inlet}$	= inlet gas temperature
TWC	= three-way catalyst
x	= longitudinal coordinate

ACKNOWLEDGEMENTS

The authors would like to thank Prof. Sergio Bova for the useful discussions and suggestions.

REFERENCES

1. Wang TJ, Baek SW, Lee JH. Kinetic parameter estimation of a diesel oxidation catalyst under actual vehicle operating conditions. *Industrial and Engineering Chemistry Research* 2008; **47**:2528–2537.
2. Abdel-Rahman AA. On the emissions from internal-combustion engines: a review. *International Journal of Energy Research* 1998; **22**:483–513.
3. Kandylas IP, Stamatelos AM. The behaviour of aged three-way catalytic converters in the different modes of legislated cycles. *International Journal of Energy Research* 2000; **24**:425–442.
4. Knafl A, Busch SB, Han M, Bohac SV, Assanis DN, Szymkowicz PG, Blint RD. Characterizing light-off behavior and species-resolved conversion efficiencies during in-situ diesel oxidation catalyst degreening. *SAE Transactions—Journal of Fuels and Lubricants* 2006; **115**:53–62; SAE paper 2006-01-0209.
5. Morea H, Hayesa RE, Liua B, Votsmeierb M, Checkel MD. The effect of catalytic washcoat geometry on light-off in monolith2001 reactors. *Topics in Catalysis* 2006; **37**(2–4):155–159.
6. Johnson TV. Diesel emission control in review. *SAE Transactions—Journal of Fuels and Lubricants* 2006; **115**:1–15; SAE paper 2006-01-0030.
7. Heywood JB. *Internal Combustion Engine Fundamentals*. McGraw Hill: New York, 1998.
8. Zheng M, Asad U, Reader GT, Tan Y, Wang M. Energy efficiency improvement strategies for a diesel engine in low-temperature combustion. *International Journal of Energy Research* 2009; **33**(1):8–28.
9. Shamim T. The effect of engine exhaust temperature modulations on the performance of automotive catalytic converters. *Journal of Engineering for Gas Turbines and Power* 2008; **130**:012801-1-9.
10. Triana A, Johnson JH, Yang SL, Baumgard KJ. An experimental and computational study on the pressure drop and regeneration characteristics of a diesel oxidation catalyst and a particulate filter. *SAE Transactions—Journal of Fuels and Lubricants* 2006; **115**:115–135; SAE paper 2006-01-0266.
11. Tauzia X, Chesse P, Hetet JF, Thouvenel N. Measurement and simulation of instantaneous emissions of a heavy truck diesel engine during transients. *Journal of Engineering for Gas Turbines and Power* 2008; **130**:012807-1-10.
12. Bhattacharyya S, Das RK. Catalytic control of automotive NO_x: a review. *International Journal of Energy Research* 1999; **23**:351–369.
13. Kandylas IP, Stamatelos AM. The behaviour of aged three-way catalytic converters in the different modes of legislated cycles. *International Journal of Energy Research* 2000; **24**:425–442.
14. Pontikakis G, Stamatelos A. Three-dimensional catalytic regeneration modeling of SiC diesel particulate filters.

Journal of Engineering for Gas Turbines and Power 2006; **128**:421–433.
15. Xu L, Graham G, McCabe RA. NO_x trap for low-temperature lean-burn-engine applications. *Catalysis Letters* 2007; **115**(3–4):108–113.
16. Kim DS, Park YJ, Lee SW, Cho YS. A study on characteristics and control strategies of cold start operation for improvement of harmful exhaust emissions in SI engines. *Journal of Mechanical Science and Technology* 2008; **22**:141–147.
17. Kowatari T, Hamada Y, Amou K, Hamada I, Funabashi H, Takakura T, Nakagome K. A study of a new aftertreatment system (1): a new dosing device for enhancing low temperature performance of urea-SCR. *SAE Transactions—Journal of Fuels and Lubricants* 2006; **115**:244–251; SAE paper 2006-01-0643.
18. Kummer JT. Catalyst for automobile emission control. *Progress in Energy and Combustion Science* 1981; **6**:177–199.
19. Burch R, Breen JP, Meunier FC. A review of the selective reduction of NO_x with hydrocarbons under lean-burn conditions with non-zeolitic oxide and platinum group metal catalyst. *Applied Catalysis B*: *Environmental* 2002; **39**:283–303.
20. Kim DS, Park YJ, Lee SW, Cho YS. A study on characteristics and control strategies of cold start operation for improvement of harmful exhaust emissions in SI engines. *Journal of Mechanical Science and Technology* 2008; **22**:141–147.
21. Zheng M, Reader GT. Energy efficiency analyses of active flow aftertreatment systems for lean burn internal combustion engines. *Energy Conversion and Management* 2004; **45**:2473–2493.
22. Güthenkea A, Chatterjeea D, Weibela M, Waldbüßera N, Kočíb P, Marekb M, Kubíčekc M. Development and application of a model for a NO_x storage and reduction catalyst. *Chemical Engineering Science* 2007; **62**:5357–5363.
23. Cauda E, Fino D, Saracco G, Specchia V. Preparation and regeneration of a catalytic diesel particulate filter. *Chemical Engineering Science* 2007; **62**:5182–5185.
24. Baik JH, Yim SD, Nam I, Mok YS, Lee JH, Cho BK, Oh SH. Control of NO_x emissions from diesel engine by selective catalytic reduction (SCR) with urea. *Topics in Catalysis* 2004; **30/31**:37–41.
25. Liu B, Hayes RE, Checkel MD, Zheng M, Mirosh E. Reversing flow catalytic converter for a natural gas/diesel dual fuel engine. *Chemical Engineering Science* 2001; **56**:2641–2658.
26. Matros YS, Bunimovich GA, Strots VO, Mirosh EA. Reversed flow converter for emission control after automotive engines. *Chemical Engineering Science* 1999; **54**:2889–2898.
27. Singh P, Thalagavara AM, Naber JD, Raux S, Dorge S, Gilot P, Climaud P, Sassi A, Johnson J, Bagley S. An experimental study of active regeneration of an advanced catalyzed particulate filter by diesel fuel injection upstream of an oxidation catalyst. *SAE Transactions—Journal of Fuels and Lubricants* 2006; **115**:334–357; SAE paper 2006-01-0879.
28. Amelio M, Morrone P. Numerical evaluation of the energetic performances of structured and random packed beds in regenerative thermal oxidizers. *Applied Thermal Engineering* 2007; **27**:762–770.
29. Amelio M, Florio G, Morrone P. Simulazione dello Scambio Termico e delle Perdite di Carico all'Interno di Rigeneratori ad Impaccamento Casuale in Ossidatori Termici Rigenerativi. *Proceedings of the '60 Congresso Nazionale ATI'*, Roma, 2005.
30. Amelio M, Florio G, Morrone P, Senatore S. The influence of rotary valve distribution systems on the energetic efficiency of regenerative thermal oxidizers (RTO). *International Journal of Energy Research* 2008; **32**:24–34.
31. Perry RH, Green DW. *Perry's Chemical Engineers' Handbook* (7th edn). McGraw Hill: New York, 1999.
32. Guglielmini G, Pisoni C. *Elementi di trasmissione del calore*. Veschi Edizioni: Milano, 1990.
33. Incropera F, De Witt D. *Fundamentals of Heat and Mass Transfer*. Wiley: U.S.A., 2002.
34. Rafidi N, Blasiak W. Thermal performance analysis on a two composite material honeycomb heat regenerators used for HiTAC burners. *Applied Thermal Engineering* 2005; **25**:2966–2982.

DOI: 10.1002/er